Fabrication and investigation on ternary heterogeneous MWCNT@TiO_2-C fillers and their silicone rubber wave-absorbing composites

Jia Zhao[a], Junliang Zhang[a,b], Lei Wang[a], Shanshan Lyu[a], Wenlong Ye[a], Ben Bin Xu[c], Hua Qiu[a], Lixin Chen[a]*, Junwei Gu[a]*

[a] MOE Key Laboratory of Material Physics and Chemistry under Extraordinary Conditions, Shaanxi Key Laboratory of Macromolecular Science and Technology, Department of Applied Chemistry, School of Chemistry and Chemical Engineering, Northwestern Polytechnical University, Xi' an, Shaanxi, 710072, P. R. China.

[b] School of Materials Science and Engineering, Henan University of Science and Technology, Luoyang, 471023, P. R. China.

[c] Department of mechanical and construction engineering, Faculty of engineering and environment, Northumbria university, Newcastle, UK, NE30 4LL

Corresponding authors, E-mail: lixin@nwpu.edu.cn (L. Chen); gjw@nwpu.edu.cn or nwpugjw@163.com (J. Gu).

Abstract

Ternary heterogeneous MWCNT@TiO_2-C wave absorbent was firstly prepared, using glucose, MWCNT, and titanium isopropoxide as raw materials, through the solvothermal process followed by post-heat treatment. Afterwards, MWCNT@TiO_2-C/silicone rubber wave-absorbing composites were fabricated *via* solution casting and subsequent curing process. XRD, Raman, XPS, and TEM analyses demonstrated the MWCNT@TiO_2-C fillers were successfully synthesized with TiO_2 and amorphous carbon coated on the surface of MWCNT. When the MWCNT@TiO_2-C/silicone rubber wave-absorbing composites contained 25 wt% MWCNT@TiO_2-C fillers and with the thickness of 2.5 mm, it displayed the minimum reflection loss of -53.2 dB and an effective absorption bandwidth of 3.1 GHz. Remarkable wave-absorbing performances for MWCNT@TiO_2-C/silicone rubber composites could be attributed to the synergetic effect of interfacial polarization loss and conduction loss.

Keywords: A. Polymer-matrix composites (PMCs); B. Electrical properties; D. Electron microscopy; E. Casting.

1. Introduction

With the fast advancement of electronic technologies, electromagnetic waves have been widely applied in the areas of advanced detectors, radio communications, and military weapons [1, 2], which causes grievous electromagnetic pollution [3, 4]. Wave-absorbing materials can effectively absorb incident electromagnetic waves, converting them into heat or other energy, and have received extensive attention [5, 6] . Wave-absorbing materials are usually composed of matrix materials (*e.g.* paraffin [7], polymers [8], and wave-transparent ceramics [9]) for the transmission of electromagnetic waves and the introduced absorbents (magnetic loss absorbents [10] and dielectric loss absorbents [11]) for the absorption of electromagnetic waves.

Magnetic loss absorbents (such as ferrites [12], carbonyl metals [13], and magnetic metals [14], *etc*) present excellent wave-absorbing performances in relatively low frequency band. However, their practical applications in wave-absorbing field are greatly restricted by high density, easy oxidation, and magnetic agglomeration [15]. Besides, the existing magnetic materials hardly have magnetic response to the high frequency band between 8.2 and 12.4 GHz [16, 17]. In comparison, dielectric loss absorbents (*e.g.*, carbon nanotube (CNT) [18], graphene [19], amorphous carbon [20], ZnO [21], $BaTiO_3$ [22], and TiO_2 [23], *etc*) have the advantages of low density, high thermal stability, and high dielectric constant value [24, 25]. CNT has attracted much attention in recent years due to its excellent electrical & thermal conductivity, and outstanding mechanical properties [26, 27]. Micheli *et al.* [28] fabricated epoxy resin (EP)/single-walled carbon nanotube (SWCNT) composites by blending-casting method. While the composites contained 3 wt% of SWCNT and with the thickness of 9.7 mm, it displayed the minimum reflection loss (RL_{min}) of -19.0 dB and an effective

absorption bandwidth (EAB) of 1.7 GHz. Kong *et al.* [29] prepared silicone resin (PDMS)/multi-walled carbon nanotube (MWCNT) composites. It was found that when the content of MWCNT was 5 wt% and the thickness was 2.75 mm, the RL_{min} and EAB of the composites were -10.0 dB and 0 GHz, respectively. It can be seen that pure single CNT is insufficient to endow the materials with high wave-absorbing ability, mainly attributed to the fact that the conductivity (σ_{dc}) of pure single CNT is too high to ensure both the real part (ε') and imaginary part (ε'') of dielectric constant ($\varepsilon_r=\varepsilon'-j\varepsilon''$) reach optimal values [30].

In order to obtain the wave-absorbing materials with ideal absorbing ability, researchers prepared wave-absorbing materials by mixing low conductivity materials with CNT as absorbents [31]. Qing *et al.* [32] fabricated MWCNT/$BaTiO_3$/EP composites employing the mixture of $BaTiO_3$ and MWCNT as absorbent. When the composites contained 0.2 vol% MWCNT and 40 vol% $BaTiO_3$ (the thickness was 1.09 mm), the corresponding RL_{min} and EAB reached -12.0 dB and 3.0 GHz, respectively. Wang *et al.* [33] prepared MWCNT/ZnO/EP composites using the mixture of nano-ZnO and MWCNT as absorbent. The corresponding RL_{min} and EAB were respectively -13.7 dB and 2.1 GHz when the composites (1.5 mm in thickness) contained 12 wt% MWCNT and 8 wt% nano-ZnO. Recent years, researchers have found that loading materials with low conductivity on the surface of CNT can further optimize the wave-absorbing performances of materials [34]. Song *et al.* [35] loaded $BaTiO_3$ on the surface of MWCNT using sol-gel method to obtain $BaTiO_3$/MWCNT hybrid materials, finally to fabricate the $BaTiO_3$/MWCNT/paraffin wave-absorbing composites. When the composites contained 70 wt% $BaTiO_3$/MWCNT (the thickness was 1.4 mm), the RL_{min} and EAB were -34.4 dB and 3.5 GHz, respectively. Song *et al.* [36] prepared ZnO/MWCNT/paraffin wave-absorbing composites from

ZnO/MWCNT hybrid materials, which was made by co-precipitation method to coat ZnO on the surface of MWCNT. The RL_{min} of the composites with 40 wt% ZnO/MWCNT (the thickness was 3.0 mm) reached -30.0 dB and the EAB almost covered the entire X-band.

TiO_2 with low conductivity and amorphous carbon in wave-absorbing field have been discovered due to their light weight, easy fabrication, and excellent chemical stability [37, 38]. Wan *et al.* [39] synthesized TiO_2@C core-shell nanocrystals by acetylene decomposition method, which was used to prepare wave-absorbing composites applying paraffin as matrix. When the thickness of the composites was 2.0 mm and contained 60 wt% of MWCNT, the RL_{min} and EAB reached -16.2 dB and 4.0 GHz, respectively. Song *et al.* [40] fabricated wave-absorbing composites with paraffin as matrix from highly ordered porous carbon (HOPC) synthesized *via* template method. When the composites contained 5 wt% HOPC and the thickness was 2.0 mm, the RL_{min} and EAB were -18.0 dB and 4.5 GHz, respectively. Nevertheless, there are few reports on the optimization of dielectric properties achieved through constructing the hetero-structures by combining CNT, TiO_2, and amorphous carbon.

In our present work, ternary heterogeneous MWCNT@TiO_2-C absorbent was prepared using titanium isopropoxide, glucose, and MWCNT as raw materials by solvothermal process followed by post-heat treatment. Afterwards, MWCNT@TiO_2-C/silicone rubber wave-absorbing composites were obtained through solution casting approach. Microstructures and morphologies for MWCNT@TiO_2-C were analyzed applying X-ray diffraction (XRD), Raman spectra, X-ray photoelectron spectroscopy (XPS), and transmission electron microscopy (TEM). In addition, the mass fraction of ternary heterogeneous MWCNT@TiO_2-C fillers affecting on the electrical conductivities, electromagnetic & wave-absorbing performances and

thermal stabilities of the MWCNT@TiO_2-C/silicone rubber composites was investigated and discussed in detail, and the relevant wave-absorbing mechanism was also preliminarily explored.

2. Experiments

2.1 Preparation of ternary heterogeneous MWCNT@TiO_2-C fillers

1 mL titanium isopropoxide, 0.08 g MWCNT, and 0.2 g glucose were uniformly dispersed in 15 mL ethanol under sonication. The reaction mixture was subsequently transferred to a 50 mL autoclave and reacted at 180°C for 40 hrs. After cooled to ambient temperature, the reaction mixture was processed by centrifuge and the obtained sludge was then washed using ethanol for several times. The obtained solid was dried at 75°C for 24 hrs, which was then heated to 500°C at a heating rate of 5°C/min and treated at 500°C for another 3 hrs under Ar atmosphere, finally to obtain the ternary heterogeneous MWCNT@TiO_2-C fillers.

2.2 Preparation of MWCNT@TiO_2-C/silicone rubber wave-absorbing composites

Silicone rubber (RTV 107) and appropriate amount of MWCNT@TiO_2-C fillers were dissolved in *n*-hexane and mechanically stirred for 24 hrs. Tetraethyl orthosilicate (5 wt% of silicone rubber) was introduced into the above mixture, followed by stirring for another 1 hr. Consequently, the reaction mixture was poured into a mold at 50°C. Finally, the obtained mixture was cured at room temperature for 24 hrs, to obtain the MWCNT@TiO_2-C/silicone rubber wave-absorbing composites. Prepared samples were named according to the amount of MWCNT@TiO_2-C used for fabricating the composites to be S0, S5, S15, S25, and S35, in responding to the content of 0 wt%, 5 wt%, 15 wt%, 25 wt%, and 35 wt%, respectively.

The information of the "Main materials" and "Characterization" details are presented

in the "Supporting Information".

3. Results and discussion

3.1 Ternary heterogeneous MWCNT@TiO_2-C fillers

Fig. 1 showed the TEM and SAED images of MWCNT and MWCNT@TiO_2-C. Pristine MWCNT displayed clear lattice fringes (**Figs. 1(a, a')**). And the corresponding SAED image (**Fig. 1(a")**) presented the diffraction rings of (002) and (101) crystal planes. For MWCNT@TiO_2-C (**Figs. 1(b, b')**), TiO_2 nanocrystals were attached onto the surface of MWCNT and amorphous carbon (around 5 nm in thickness) was covered on the outermost layer of MWCNT@TiO_2-C. Meanwhile, apart from the diffraction rings of MWCNT, diffraction rings of anatase TiO_2 (004) and (200) crystal planes also appeared (**Fig. 1(b")**), indicating TiO_2 nanocrystals were sandwiched between outer amorphous carbon and inner MWCNT [41]. On one hand, glucose could promote the *in*-situ growth of TiO_2 nanocrystals onto the surface of MWCNT. On the other hand, amorphous carbon from the carbonization of glucose could restrict the growth of TiO_2 nanocrystals during solvothermal and annealing process. Consequently, the nano-sized TiO_2 crystals were generated [42]. As shown in **Figs. 1(b'-1, b'-2, and b'-3)**, MWCNT@TiO_2-C possessed multiple heterogeneous interfaces, beneficial to the attenuation of electromagnetic waves induced by interfacial polarization [43].

XRD patterns of MWCNT and MWCNT@TiO_2-C were shown in **Fig. 2(a)**. MWCNT presented the peak (002) of graphite at 26.4° [44]. In comparison, apart from the peak (002), the diffraction peaks at 25.3°, 37.8°, 48.0°, 54.8°, 62.6°, 68.8°, 70.3°, and 75.2° in respective to the (101), (004), (200), (211), (204), (116), (220), and (215) crystal planes of anatase TiO_2 also appeared for MWCNT@TiO_2-C, suggesting the TiO_2 nanocrystals were successfully introduced onto the surface of MWCNT. Moreover,

the wide background peak (in the region of 20-35°) observed for MWCNT@TiO_2-C indicated the existence of amorphous carbon layers. **Fig. 2(b)** depicted the Raman spectra of MWCNT and MWCNT@TiO_2-C. Both D peak at 1347 cm^{-1} (disordered carbon) and G peak at 1580 cm^{-1} (sp^2 hybrid graphite carbon) were observed for MWCNT. In addition to the D and G peaks, the characteristic peaks of anatase TiO_2 at 395 (B_{1g}), 513 (A_{1g}), and 635 cm^{-1} (E_g) appeared as well for MWCNT@TiO_2-C [45]. According to Gaussian-Lorentzian fitting, the intensity ratio of D-band/G-band (I_D/I_G) for MWCNT was 0.2, whereas the corresponding I_D/I_G of MWCNT@TiO_2-C was 0.5. This was mainly because the carbon layer decorated on MWCNT@TiO_2-C was amorphous [41]. In addition, the existence of TiO_2 could also reduce the sp^2 carbon domains of MWCNT [46]. In **Fig. 2(c)**, the peaks at 283.1, 532.4, and 978.8 eV observed for MWCNT respectively corresponded to C 1s, O 1s, and O KLL, revealing C and O in MWCNT, consistent with the result of **Fig. S1**. For MWCNT@TiO_2-C, the characteristic peaks of Ti at 35.6 (Ti 3p), 60.9 (Ti 3s), 458.4 (Ti 2p), and 565.0 (Ti 2s) eV also appeared. In **Fig. 2(c')**, MWCNT consisted of the peaks at 532.0, 532.8, and 533.8 eV, respectively corresponding to C=O, COO-, and C-OH [47, 48]. These oxygen-containing functional groups ensured the homogeneous dispersion of MWCNT in ethanol, beneficial to the formation of MWCNT@TiO_2-C. Compared with MWCNT, the new peak of O 1s (**Fig. 2(c")**) at 530.6 eV and the peaks of Ti 2p (**Fig. 2(c"')**) at 459.3 and 464.8 eV observed for MWCNT@TiO_2-C revealed the success formation of TiO_2 on the surface of MWCNT [49].

3.2 MWCNT@TiO_2-C/silicone rubber wave-absorbing composites

Fig. 3(a) showed the effect of MWCNT@TiO_2-C content on the electrical conductivity (σ_{dc}) values of the MWCNT@TiO_2-C/silicone rubber wave-absorbing composites. The σ_{dc} value of pure silicone rubber (S0) was only 6.5×10^{-10} S/m. While

the amount of MWCNT@TiO_2-C fillers was 5 wt% (S5), the σ_{dc} value reached up to 9.9×10^{-4} S/m. As the content of MWCNT@TiO_2-C fillers further increased to 35 wt% (S35), the corresponding σ_{dc} value reached the maximum of 0.6 S/m. This was because the MWCNT@TiO_2-C fillers were randomly distributed inner silicone rubber matrix at lower MWCNT@TiO_2-C content. Therefore, a small amount of conductive channels was formed, resulting in the increase of the σ_{dc} value. With the further introduction of MWCNT@TiO_2-C fillers, more effectively conductive networks were formed, leading the further increase of σ_{dc} value [50]. **Fig. 3(b)** presented the complex permeability ($\mu_r=\mu'-j\mu''$) of the MWCNT@TiO_2-C/silicone rubber wave-absorbing composites. For all composites, the real part (μ') and imaginary part (μ'') approximated to 1 and 0, respectively. And there was no obvious change for μ' and μ'' in the whole X-band (Permeability was mainly reflected in the low frequency band, and materials hardly had magnetic response in the high frequency band). As a result, the magnetic properties and losses of our fabricated composites could be ignored. The complex permittivity ($\varepsilon_r=\varepsilon'-j\varepsilon''$) and dielectric loss tangent (tanδ) values of the composites were depicted in **Figs. 3(c-f)**. The average values of real part (ε'), imaginary part (ε''), and loss tangent (tanδ) for S0 was 2.88, 0.07, and 0.02, respectively. With increasing the mass fraction of MWCNT@TiO_2-C fillers, ε', ε'', and tanδ values all showed incremental trend. For instance, the average values of ε' increased to 4.21, 5.74, 8.29, and 11.57 for S5, S15, S25, and S35, respectively, while the average values of ε'' increased to 1.03, 1.93, 3.13, and 5.08, respectively. Besides, the average value of tanδ was increased to 0.25, 0.34, 0.38, and 0.44, respectively. Firstly, with increasing the addition of MWCNT@TiO_2-C fillers, more effectively conductive networks were formed (**Fig. 3(a)**), which would improve the dielectric properties of the composites. Secondly, introducing the MWCNT@TiO_2-C fillers

could generate many heterogeneous interfaces. Under the external electromagnetic field, the charges would accumulate at the heterogeneous interfaces and result in the interfacial polarization relaxation, which would improve the dielectric properties [51]. Polarization relaxation could be studied *via* Debye relaxation theory (**Eq.1**), and the plot of ε' versus ε'' would be one single semicircle (Cole-Cole semicircle), in which each semicircle represented one Debye relaxation process [29].

$$\left(\varepsilon' - \frac{\varepsilon_s - \varepsilon_\infty}{2}\right)^2 + \left(\varepsilon''\right)^2 = \left(\frac{\varepsilon_s - \varepsilon_\infty}{2}\right)^2 \quad \textbf{(Eq.1)}$$

Where ε_∞ and ε_s represent relative dielectric permittivity at high frequency limit and static permittivity, respectively.

Fig. 4 demonstrated the Cole-Cole curves of the MWCNT@TiO_2-C/silicone rubber wave-absorbing composites (S5-S35). There was no obvious Cole-Cole semicircle for S5, which was mainly attributed that the content of MWCNT@TiO_2-C fillers was too low to have obvious effects on the dielectric properties of the composites. However, there were at least four obvious Cole-Cole semicircles in S15, S25, and S35, corresponding from many heterogeneous interfaces (interfaces between MWCNT and amorphous carbon, MWCNT and TiO_2, TiO_2 and amorphous carbon, and amorphous carbon and silicone rubber).

Fig. 5(a) demonstrated the reflection loss (RL, calculated according to **Eqs. S1-2**) values of the MWCNT@TiO_2-C/silicone rubber wave-absorbing composites (S0-S35) with the thickness of 2.5 mm at X-band. Wave-absorbing performance of S0 was very poor. With increasing the amount of MWCNT@TiO_2-C fillers, the wave-absorbing ability of the composites increased firstly before showing a decreased trend. When the content of MWCNT@TiO_2-C fillers was 25 wt%, the composites exhibited the optimal wave-absorbing performance by showing the minimum RL_{min} of -53.2 dB and

EAB of 3.1 GHz. Firstly, the impedance matching of MWCNT@TiO_2-C fillers could reduce the electromagnetic waves on the surface of the composites, to ensure the unhindered entry of electromagnetic waves [52]. Secondly, the dielectric loss generated by MWCNT@TiO_2-C/silicone rubber wave-absorbing composites could attenuate electromagnetic waves that entered the composites [53]. However, with the further addition of MWCNT@TiO_2-C fillers, the deviated dielectric constant of S35 from the optimal value caused the impedance difference, which would result in strong electromagnetic waves reflecting on the surface of the composites [53]. Therefore, the wave-absorbing performance was deteriorated and the respective RL_{min} and EAB were only -24.0 dB and 1.95 GHz, respectively.

Fig. 5(b) showed the RL values of the MWCNT@TiO_2-C/silicone rubber wave-absorbing composites S25 with various thicknesses. While the thickness of the sample was less than 2.5 mm, the wave-absorbing performances of S25 were gradually improved as the thickness increased. As the thickness reached 2.5 mm, the composite exhibited the optimal wave-absorbing performance, with the RL_{min} and EAB being -53.2 dB and 3.1 GHz, respectively. However, when the thickness was more than 2.5 mm, the corresponding wave-absorbing performance of S25 gradually deteriorated. This phenomenon was attributed to the destructive interference effects. While the thickness was an odd time of a quarter of wavelength, the reflected wave phase of upper surface was inverse to that of bottom surface, thus resulting in the destructive interference effects and the effective improvement of wave-absorbing performance [52]. In our work, 2.5 mm was an odd time of a quarter of wavelength, which thus resulted in the optimal wave-absorbing ability. Compared to the wave-absorbing performances for the composites reported in other works (**Table S2**), our fabricated MWCNT@TiO_2-C/silicone rubber wave-absorbing composites also

demonstrated the optimal wave-absorbing performance.

4. Conclusions

XRD, Raman, XPS, and TEM analyses demonstrated the ternary heterogeneous MWCNT@TiO_2-C fillers were successfully synthesized. When the MWCNT@TiO_2-C/silicone rubber wave-absorbing composites contained 25 wt% MWCNT@TiO_2-C fillers and with the thickness of 2.5 mm, it displayed the minimum reflection loss of -53.2 dB and the corresponding effective absorption bandwidth of 3.1 GHz. Remarkable wave-absorbing ability was mainly attributed to the synergetic effect of interfacial polarization loss and conduction loss. Our fabricated MWCNT@TiO_2-C/silicone rubber wave-absorbing composites possess potential applications in the field of electromagnetic protection.

Acknowledgement

This work is supported by Shanghai Aerospace Science and Technology Innovation Fund (2017-121); Shenzhen Science and Technology Innovation Fund (JCYJ20170815155705061); Space Supporting Fund from China Aerospace Science and Industry Corporation (2019-HT-XG); Open Fund from Henan University of Science and Technology.

References

[1] H. Lv, Z. Yang, P. Wang, G. Ji, J. Song, L. Zheng, H. Zeng, Z. Xu, A voltage-boosting strategy enabling a low-frequency, flexible electromagnetic wave absorption wave absorption device, Adv. Mater. 30 (2018) 1706343.

[2] (a) N. Wu, J. Qiao, J. Liu, W. Du, D. Xu, W. Liu, Strengthened electromagnetic absorption performance derived from synergistic effect of carbon nanotube hybrid with Co@C beads, Adv. Compos. Hybrid. Mater. 1 (1) (2018) 149-159. (b) L. Lv, J. Liu, C. Liang, J. Gu, H. Liu, C. Liu, Y. Lu, K. Sun, R. Fan, N. Wang, N. Lu, Z. Guo,

An overview of electrically conductive polymer nanocomposites toward electromagnetic interference shielding, Eng. Sci. 2 (2018) 26-42.

[3] J. Liu, H. Liang, Y. Zhang, G. Wu, H. Wu, Facile synthesis of ellipsoid-like $MgCo_2O_4/Co_3O_4$ composites for strong wideband microwave absorption application, Compos. Part B-Eng. 176 (2019) 107240.

[4] Y. Chen, Z. Huang, M. Lu, W. Cao, J. Yuan, D. Zhang, M. Cao, 3D Fe_3O_4 nanocrystals decorating carbon nanotubes to tune electromagnetic properties and enhance microwave absorption capacity, J. Mater. Chem. A 3 (2015) 12621-12625.

[5] Z. Jia, Z. Gao, A. Feng, Y. Zhang, C. Zhang, G. Nie, K. Wang, G. Wu, Laminated microwave absorbers of A-site cation deficiency perovskite $La_{0.8}FeO_3$ doped at hybrid RGO carbon, Compos. Part B-Eng. 176 (2019) 107246.

[6] H. Liang, J. Liu, Y. Zhang, L. Luo, H. Wu, Ultra-thin broccoli-like SCFs@TiO_2 one-dimensional electromagnetic wave absorbing material, Compos. Part B-Eng. 178 (2019) 107507.

[7] B. Wen, X. Wang, W. Cao, H. Shi, M. Lu, G. Wang, H. Jin, W. Wang, J. Yuan, M. Cao, Reduced graphene oxides: the thinnest and most lightweight materials with highly efficient microwave attenuation performances of the carbon world, Nanoscale 6 (2014) 5754-5761.

[8] M. Oyharcabal, T. Olinga, M. Foulc, S. Lacomme, E. Gontier, V. Vigneras, Influece of the morphology of polyaniline on the microwave absorption properties of epoxy polyaniline composites, Compos. Sci. Technol. 74 (2013) 107-112.

[9] Y. Liu, Y. Feng, H. Gong, Y. Zhang, X. Lin, B. Xie, J. Mao, Electromagnetic wave absorption properties of nickel-containing polymer-derived SiCN ceramics, Ceram. Int. 44 (2018) 10945-10950.

[10] B. Zhao, J. Deng, R. Zhang, L. Liang, B. Fan, Z. Bai, G. Shao, C. Park, Recent

advances on the electromagnetic wave absorption properties of Ni based materials, Eng. Sci. 3 (2018) 5-40.

[11] (a) Y. Wei, Y. Shi, Z. Jiang, X. Zhang, H. Chen, Y. Zhang, J. Zhang, C. Gong, High performance and lightweight electromagnetic wave absorbers based on TiN/RGO flakes, J. Alloy. Compd. 810 (2019) 151950. (b) H. Wang, K. Zhu, L. Yan, C. Wei, Y. Zhang, C. Gong, J. Guo, J. Zhang, D. Zhang, J. Zhang, Efficient and Scalable High-Quality Graphene Nanodot Fabrication through Confined Lattice Plane Electrochemical Exfoliation, Chem Commun 55 (2019) 5805-5808.

[12] G. Tong, W. Wu, J. Guan, H. Qian, J. Yuan, W. Li, Synthesis and characterization of nanosized urchin-like α-Fe_2O_3 and Fe_3O_4: microwave electromagnetic and absorbing properties, J. Alloy. Compd. 509 (2011) 4320-4326.

[13] Z. Zhu, X. Sun, H. Xue, X. Fan, X. Pan, J. He, Graphene-carbonyl iron cross-linked composites with excellent electromagnetic wave absorption properties, J. Mater. Chem. C 2 (2014) 6582-6591.

[14] Z. Li, X. Han, Y. Ma, D. Liu, Y. Wang, P. Xu, C. Li, Y. Du, MOFs-derived hollow Co/C microspheres with enhanced microwave absorption performance, ACS Sustain. Chem. Eng. 6 (2018) 8904-8913.

[15] Q. Liu, Q. Cao, H. Bi, C. Liang, K. Yuan, W. She, Y. Yang, R. Che, CoNi@SiO_2@TiO_2 and CoNi@air@TiO_2 microspheres with strong wideband microwave absorption, Adv. Mater. 28 (2016) 486-490.

[16] C. Luo, W. Duan, X. Yin, J. Kong, Microwave-absorbing polymer-derived ceramics from cobalt-coordinated poly(dimethylsilylene)diacetylenes, J. Phy. Chem. C 120 (2016) 18721-18732.

[17] X. Liu, Y. Chen, C. Hao, J. Ye, R. Yu, D. Huang, Graphene-enhanced microwave absorption properties of Fe_3O_4/SiO_2 nanorods, Compos. Part A-Appl. 89 (2016)

40-46.

[18] (a) Y. Huangfu, K. Ruan, H. Qiu, Y. Lu, C. Liang, J. Kong, J. Gu, Fabrication and investigation on the PANI/MWCNT/thermally annealed graphene aerogel/epoxy electromagnetic interference shielding nanocomposites, Compos. Part A-Appl. 121 (2019) 265-272. (b) Y. Guo, K. Ruan, X. Yang, T. Ma, J. Kong, N. Wu, J. Zhang, J. Gu, Z. Guo, Constructing fully carbon-based fillers with hierarchical structure to fabricate highly thermally conductive polyimide nanocomposites, J. Mater. Chem. C 7 (2019) 7035-7044.

[19] (a) X. Yang, S. Fan, Y. Li, Y. Guo, Y. Li, K. Ruan, S. Zhang, J. Zhang, J. Kong, J. Gu, Synchronously improved electromagnetic interference shielding and thermal conductivity for epoxy nanocomposites by constructing 3D copper nanowires/thermally annealed graphene aerogel framework, Compos. Part A-Appl. 128 (2020) 105670. (b) C. Liang, P. Song, H. Qiu, Y. Zhang, X. Ma, F. Qi, H. Gu, J. Kong, D. Cao, J. Gu, Constructing interconnected spherical hollow conductive networks in silver platelets/reduced graphene oxide foam/epoxy nanocomposites for superior electromagnetic interference shielding effectiveness, Nanoscale, 2019, DOI: 10.1039/C9NR06022G.

[20] P. Xie, H. Li, B. He, F. Dang, J. Lin, R. Fan, C. Hou, H. Liu, J. Zhang, Y. Ma, Z. Guo, Bio-gel derived nickel/carbon nanocomposites with enhanced microwave absorption, J. Mater. Chem. C 6 (2018) 8812-8822.

[21] L. Zhou, W. Zhou, T. Liu, F. Luo, D. Zhu, Influence of ZnO content and annealing temperature on the dielectric properties of ZnO/Al_2O_3 composite coating, J. Alloy. Compd. 509 (2011) 5903-5907.

[22] L. Tian, X. Yan, J. Xu, P. Wallenmeyer, J. Murowchick, L. Liu, X. Chen, Effect of hydrogenation on the microwave absorption properties of $BaTiO_3$ nanoparticles, J.

Mater. Chem. A 3 (2015) 12550-12556.

[23] T. Xia, C. Zhang, N. Oyler, X. Chen, Hydrogenated TiO_2 nanocrystals: a novel microwave absorbing material, Adv. Mater. 25 (2013) 6905-6910.

[24] Y. Zhang, Y. Huang, T. Zhang, H. Chang, P. Xiao, H. Chen, Z. Huang, Y. Chen, Broadband and tunable high-performance microwave absorption of an ultralight and highly compressible graphene foam, Adv. Mater. 27 (2015) 2049-2053.

[25] K. Ruan, Y. Guo, Y. Tang, Y. Zhang, M. He, J. Gu, Improved thermal conductivities in polystyrene nanocomposites by incorporating thermal reduced graphene oxide via electrospinning-hot press technique, Compos. Commun. 10 (2018) 68-72

[26] J. Schnorr, T. Swager, Emerging applications of carbon nanotubes, Chem. Mater. 23 (2010) 646-657.

[27] R. Dileo, A. Castiglia, M. Ganter, R. Rogers, C. Cress, R. Raffaelle, B. Landi, Enhanced capacity and rate capability of carbon nanotube based anodes with titanium contacts for lithium ion batteries, ACS Nano 4 (2010) 6121-6131.

[28] D. Michell, C. Apollo, R. Pastore, M. Marchetti, X-band microwave characterization of carbon-based nanocomposite material, absorption capability comparison and RAS design simulation, Compos. Sci. Technol. 70 (2010) 400-409.

[29] L. Kong, X. Yin, X. Yuan, Y. Zhang, X. Liu, L. Cheng, L. Zhang, Electromagnetic wave absorption properties of graphene modified with carbon nanotube/poly (dimethyl siloxane) composites, Carbon 73 (2014) 185-193.

[30] I. Huynen, N. Quiévy, C. Bailly, P. Bollen, C. Detrembleur, S. Eggermont, I. Molenberg, J. Thomassin, L. Urbanczyk, T. Pardoen, Multifunctional hybrids for electromagnetic absorption, Acta Mater. 59 (2011) 3255-3266.

[31] H. Li, J. Wang, Y. Huang, X. Yan, J. Qi, J. Liu, Y. Zhang, Microwave absorption

properties of carbon nanotubes and tetrapod-shaped ZnO nanostructures composites, Mat. Sci. Eng. B 175 (2010) 81-85.

[32] Y. Qing, X. Wang, Y. Zhou, Z. Huang, F. Luo, W. Zhou, Enhanced microwave absorption of multi-walled carbon nanotubes/epoxy composites incorporated with ceramic particles, Compos. Sci. Technol. 102 (2014) 161-168.

[33] J. Wang, H. Li, Y. Huang, H. Yu, Y. Zhang, Microwave absorbing properties of composites coating by carbon nanotube and nanoscaled tetrapod-shaped ZnO, Acta Phys. Sin. 59 (2010) 1946-1951.

[34] F. Wu, Y. Xia, Y. Wang, M. Wang, Two-step reduction of self-assembed three-dimensional (3D) reduced graphene oxide (RGO)/zinc oxide (ZnO) nanocomposites for electromagnetic absorption, J. Mater. Chem. A 2 (2014) 20307-20315.

[35] Y. Song, J. Zheng, X. Liu, M. Sun, S. Zhao, Facile synthesis of $BaTiO_3$ on multiwalled carbon nanotubes as a synergistic microwave absorber, J. Mater. Sci-Mater. El. 27 (2016) 3390-3396.

[36] W. Song, M. Cao, B. Wen, Z. Hou, J. Cheng, J. Yuan, Synthesis of zinc oxide particles coated multiwalled carbon nanotubes: dielectric properties, electromagneic interference shielding and microwave absorption, Mater. Res. Bull. 47 (2012) 1747-1754.

[37] R. Qiang, Y. Du, Y. Wang, N. Wang, C. Tian, J. Ma, P. Xu, X. Han, Rational design of yolk-shell C@C microspheres for the effective enhancement in microwave absorption, Carbon 98 (2016) 599-606.

[38] H. Miyazaki, T. Matsuura, T. Ota, TiO_2 nano-particles based photochromic composite films, Compos. Commun. 10 (2018) 136-139.

[39] G. Wan, L. Yu, X. Peng, G. Wang, X. Huang, H. Zhao, Y. Qin, Preparation and

microwave absorption properties of uniform TiO_2@C core-shell nanocrystals, RSC Adv. 5 (2015) 77443-77448.

[40] W. Song, M. Cao, L. Fan, M. Lu, Y. Li, C. Wang, H. Ju, Highly ordered porous carbon/wax composites for effective electromagnetic attenuation and shielding, Carbon 77 (2014) 130-142.

[41] B. Wang, H. Xin, X. Li, J. Cheng, G. Yang, F. Nie, Mesoporous CNT@TiO_2-C nanocable with extremely durable high rate capability for lithium-ion battery anodes, Sci. Rep. 4 (2014) 3729.

[42] D. Wang, J. Yang, X. Li, D. Geng, R. Li, M. Cai, T. Sham, X. Sun, Layer by layer assembly of sandwiched graphene/SnO_2 nanorod/carbon nanostructures with ultrahigh lithium ion storage properties, Energy Environ. Sci. 6 (2013) 2900-2906.

[43] J. Zhao, Y. Lu, W. Ye, L. Wang, B. Liu, S. Lv, L. Chen, J. Gu, Enhanced wave-absorbing performances of silicone rubber composites by incorporating C-SnO_2-MWCNT absorbent with ternary heterostructure, Ceram. Int. 45 (2019) 20282-20289.

[44] W. Duan, X. Yin, C. Luo, J. Kong, F. Ye, H. Pan, Microwave-absorption properties of SiOC ceramics derived from novel hyperbranched ferrocene-containing polysiloxane, J. Eur. Ceram. Soc. 37 (2017) 2021-2030.

[45] F. Cao, Y. Guo, S. Zheng, X. Wu, L. Jiang, R. Bi, L. Wan, J. Maier, Symbiotic coaxial nanocables: facile synthesis and an efficient and elegant morphological solution to the lithium storage problem, Chem. Mater. 22 (2010) 1908-1914.

[46] S. Wang, L. Shi, G. Chen, C. Ba, Z. Wang, J. Zhu, Y. Zhao, M. Zhang, S. Yuan, In situ synthesis of tungsten-doped SnO_2 and graphene nanocomposites for high-performance anode materials of lithium-ion batteries, ACS Appl. Mater. Interfaces 9 (2017) 17163-17171.

[47] C. Ma, W. Zhang, Y. He, Q. Gong, H. Che, Z. Ma, Carbon coated SnO_2 nanoparticles anchored on CNT as a superior anode material for lithium-ion batteries, Nanoscale 8 (2016) 4121-4126.

[48] Y. Cheng, J. Huang, H. Qi, L. Cao, X. Luo, J. Li, Z. Xu, J. Yang, Controlling the Sn-C bonds content in SnO_2@CNTs composites to form in situ pulverized structure for enhanced electrochemical kinetics, Nanoscale 9 (2017) 18681-18689.

[49] X. Yue, S. Yi, R. Wang, Z. Zhang, S. Qiu, Cobalt phosphide modified titanium oxide nanophotocatalysts with significantly enhanced photocatalytic hydrogen evolution from water splitting, Small 13 (2017) 1603301-1603309.

[50] L. Wang, L. Chen, P. Song, C. Liang, Y. Lu, H. Qiu, Y. Zhang, J. Kong, J. Gu, Fabrication on the annealed Ti_3C_2Tx MXene/Epoxy nanocomposites for electromagnetic interference shielding application, Compos. Part B-Eng. 171 (2019) 111-118.

[51] X. Liu, X. Cui, Y. Chen, X. Zhang, R. Yu, G. Wang, H. Ma, Modulation of electromagnetic wave absorption by carbon shell thickness in carbon encapsulated magnetite nanospindles-poly(vinylidene fluoride) composites, Carbon 95 (2015) 870-878.

[52] L. Kong, X. Yin, F. Ye, Q. Li, L. Zhang, L. Cheng, Electromagnetic wave absorption properties of ZnO-based materials modified with $ZnAl_2O_4$ nanograins, J. Phys. Chem. C 117 (2013) 2135-2146.

[53] W. Feng, Y. Wang, J. Chen, L. Wang, L. Guo, J. Ouyang, D. Jia, Y. Zhou, Reduced graphene oxide decorated with in-situ growing ZnO nanocrystals: facile synthesis and enhanced microwave absorption properties, Carbon 108 (2016) 52-60.

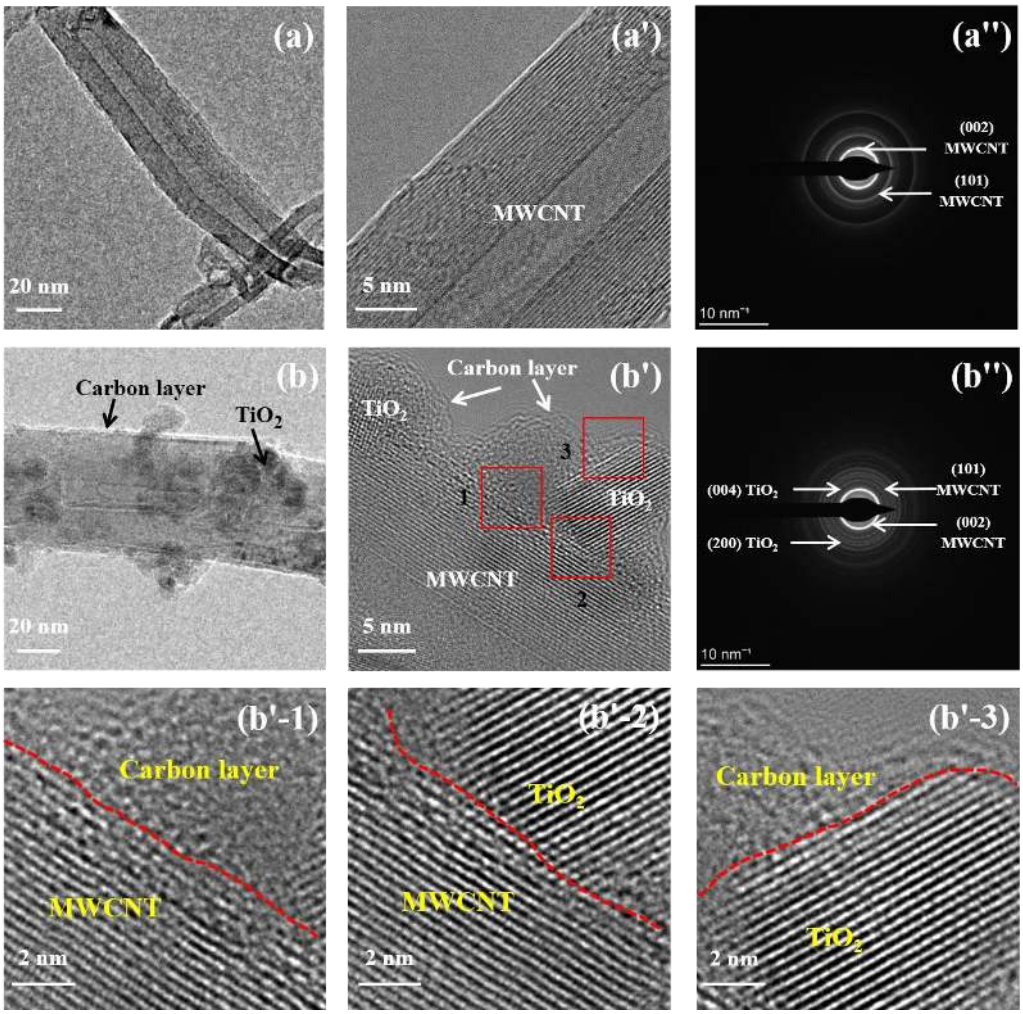

Fig. 1 TEM images of MWCNT (a) and MWCNT@TiO_2-C (b); HRTEM images of MWCNT (a') and MWCNT@TiO_2-C (b'); SAED patterns of MWCNT (a'') and MWCNT@TiO_2-C (b''); b'-1, b'-2, and b'-3 represent the magnified TEM images of regions marked with red rectangles 1, 2, and 3 in b', respectively.

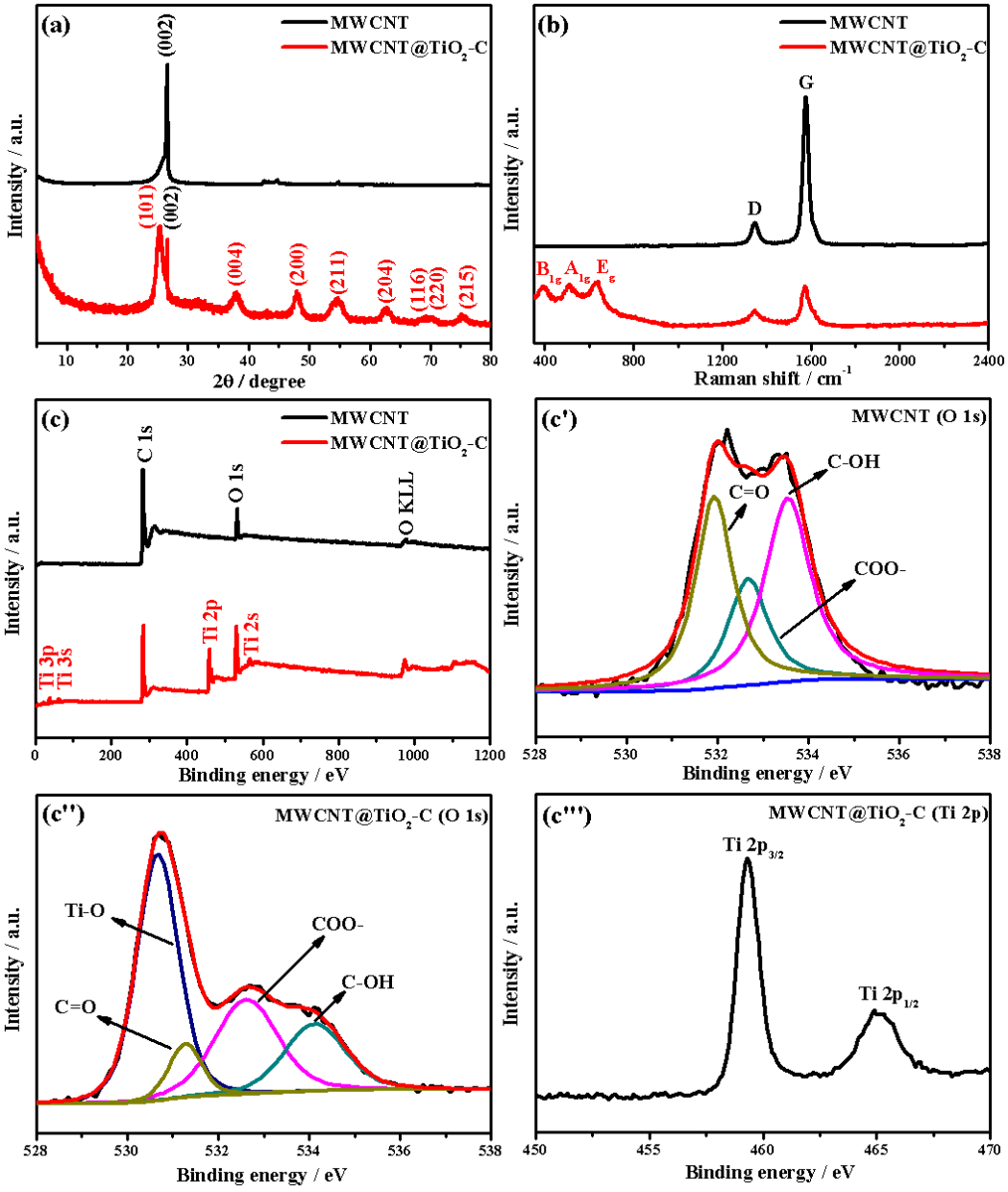

Fig. 2 XRD (a), Raman (b), and XPS wide-scan spectra (c) of MWCNT and MWCNT@TiO_2-C; O 1s high resolution XPS spectra of MWCNT (c') and MWCNT@TiO_2-C (c''); Ti 2p high resolution XPS spectra of MWCNT@TiO_2-C (c''').

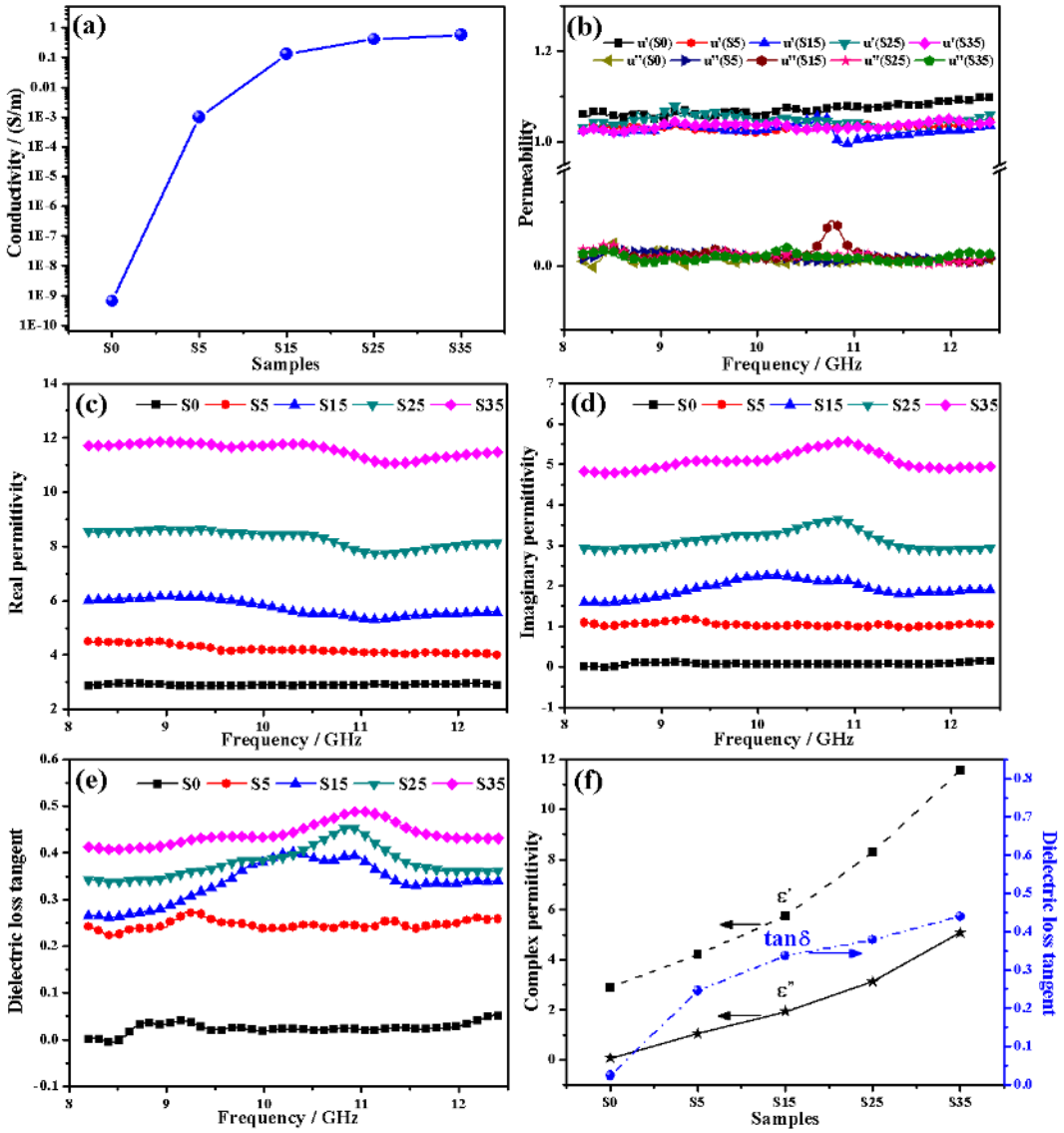

Fig. 3 Electrical conductivity (a), complex permeability (b), real permittivity (c), imaginary permittivity (d), dielectric loss tangent (e), and average value of complex permittivity (f) for MWCNT@TiO_2-C/silicone rubber wave-absorbing composites.

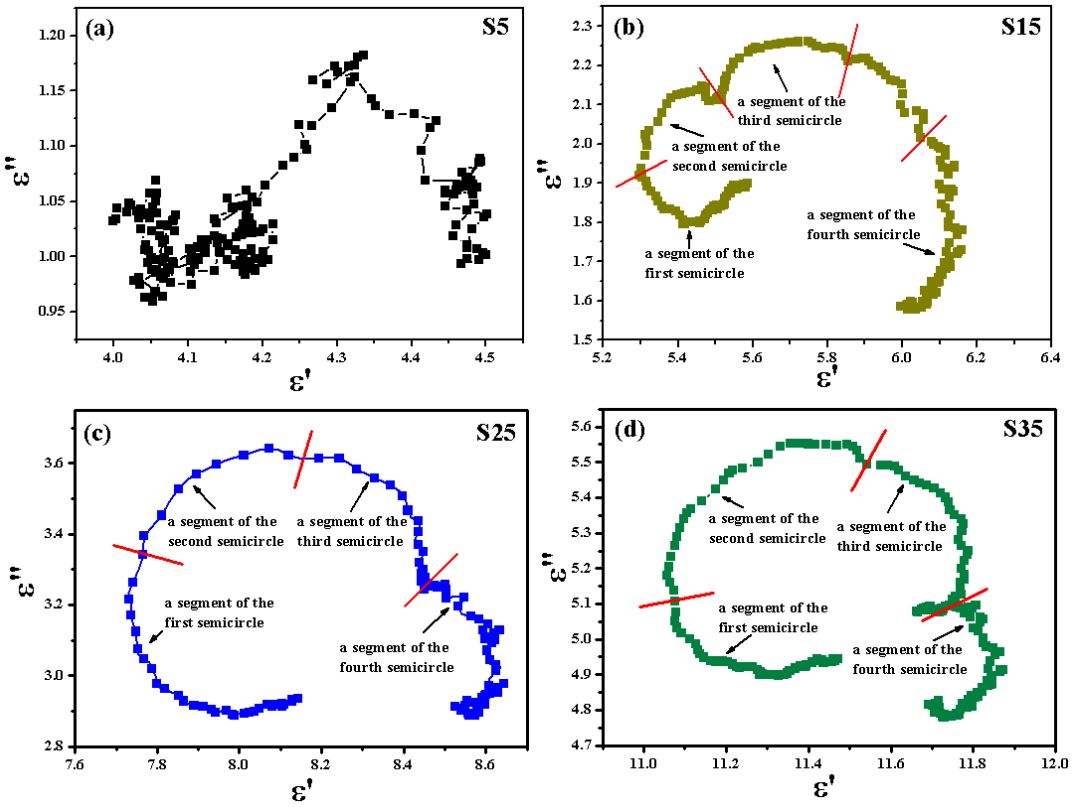

Fig. 4 Cole-Cole curves of MWCNT@TiO_2-C/silicone rubber wave-absorbing composites (S5-S35).

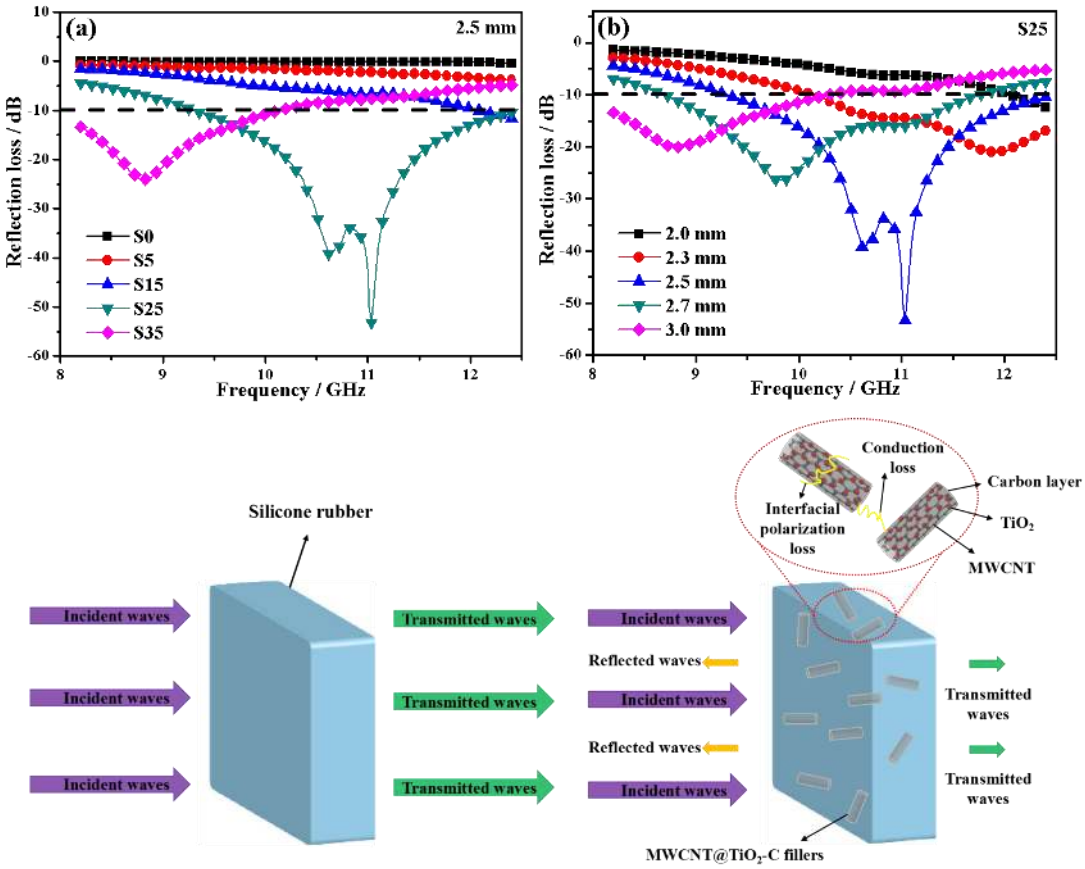

Fig. 5 Reflection loss values of the MWCNT@TiO_2-C/silicone rubber wave-absorbing composites (a); Reflection loss values for S25 with different thicknesses (b); Schematic illustration of electromagnetic waves absorption mechanism (c).

Conflict of Interest

We wish to confirm that there are no known conflicts of interest associated with this publication and there has been no significant financial support for this work that could have influenced its outcome.

We confirm that the manuscript has been read and approved by all named authors and that there are no other persons who satisfied the criteria for authorship but are not listed. We further confirm that the order of authors listed in the manuscript has been approved by all of us.

We confirm that we have given due consideration to the protection of intellectual property associated with this work and that there are no impediments to publication, including the timing of publication, with respect to intellectual property. In so doing we confirm that we have followed the regulations of our institutions concerning intellectual property.

We understand that the Corresponding Author is the sole contact for the Editorial process (including Editorial Manager and direct communications with the office). Junwei Gu is responsible for communicating with the other authors about progress, submissions of revisions and final approval of proofs. We confirm that we have provided a current, correct email address which is accessible by the Corresponding Author and which has been configured to accept email from gjw@nwpu.edu.cn & nwpugjw@163.com.

Signed by all authors as follows:

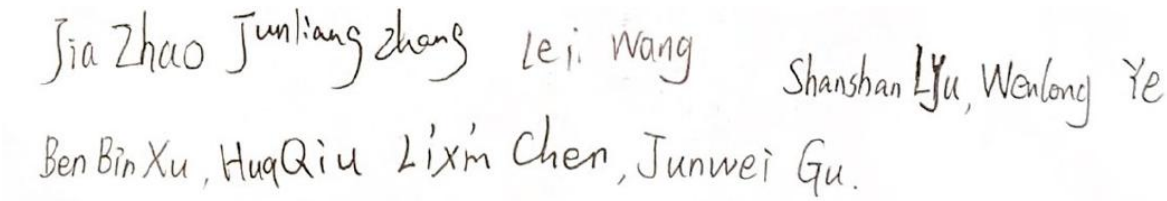

Author Contribution Statement

Jia Zhao: Conceptualization, Fabrication on the MWCNT@TiO_2-C fillers, Writing- Original draft preparation

Junliang Zhang: Composites fabrication, Writing- Original draft preparation

Lei Wang: Mechanism analysis

Shanshan Lyu: Methodology

Wenlong Ye: Data curation

Ben Bin Xu: Writing- Reviewing and Editing

Hua Qiu: Performance tests

Lixin Chen: Supervision

Junwei Gu: Supervision